Local magnetic behavior across the first order phase transition in
La(Fe0.9Co0.015Si0.085)13 magneto caloric compound

(Article begins on next page)

19 September 2024

Corresponding Author: Dr. Cecilia Bennati,

Corresponding Author's Institution: Politecnico di Torino

First Author: Cecilia Bennati

Order of Authors: Cecilia Bennati; Francesco Laviano; Gianfranco Durin; Elena Sonia Olivetti; Vittorio Basso; Gianluca Ghigo; Michaela Kuepferling

Abstract: We visualize, with a magneto optical imaging technique with indicator film, the local magnetic response of the compound La(Fe0.9Co0.015Si0.085)13 during its first order magneto structural transition. The technique allowed to compare the stray fields of the main magneto caloric phase and of secondary phases present in the sample, thus to obtain the magnetic behaviour of each above and below the Curie temperature with respect the surrounds. Computing the change in the total magnetic flux, when the sample crosses the Curie point, both in cooling and heating, we are finally able to correlate the average thermal hysteresis of the transition with the local magnetic properties at single sites and analyse the influence of defects on the transition dynamics.

*Cover Letter

Dear editor,

this paper is a submission for manuscripts associated with oral presentations of the 20th International Conference on Magnetism.

I provide the informations received about the manuscript.

      paper number : 2189.00

      presentation type: Oral presentation

      topic: 02. Spin Systems & Magnetic Structures

      subtopic: 02.07. Magnetic phase transitions and magnetic interactions

Best regards,

Cecilia Bennati

Local magnetic behaviour across the first order phase transition in $La(Fe_{0.9}Co_{0.015}Si_{0.085})_{13}$ magneto caloric compound

C. Bennati[a,b,], F. Laviano[a], G. Durin[b], E.S. Olivetti[b], V. Basso[b], G.Ghigo[a], and M. Kuepferling[b]

[a]*Department of Applied Science and Technology, Politecnico di Torino, C.so Duca degli Abruzzi 24, 10129 Turin, Italy*
[b]*Istituto Nazionale di Ricerca Metrologica (INRIM), Strada delle Cacce 91, 10135 Turin, Italy*

Abstract

We visualize, with a magneto optical imaging technique with indicator film, the local magnetic response of the compound $La(Fe_{0.9}Co_{0.015}Si_{0.085})_{13}$ during its first order magneto structural transition. The technique allowed to compare the stray fields of the main magneto caloric phase and of secondary phases present in the sample, thus to obtain the magnetic behaviour of each above and below the Curie temperature with respect the surrounds. Computing the change in the total magnetic flux, when the sample crosses the Curie point, both in cooling and heating, we are finally able to correlate the average thermal hysteresis of the transition with the local magnetic properties at single sites and analyse the influence of defects on the transition dynamics.

Keywords:
magneto-caloric, magneto optic, phase transition, dynamics, micro structure

1. Introduction

In the framework of solid state refrigeration, the last 30 years have been dedicated to the study of magneto-caloric compounds [1]. The magneto-caloric effect (MCE) origins from the change in the entropy of a system when forced by a magnetic field; in isothermal conditions the entropy change (ΔS_{iso}) results in an exchange of heat of the material which can be used to increase/decrease the temperature of the system [2]. Magnetic materials which shows a large MCE can give rise to temperature gradients up to 7 K with a 2 Tesla magnetic field [3]. These large magneto caloric effects are possible when, under the effect of an external magnetic field, a material undergoes a phase transition which involves changes both in the intrinsic magnetic order and structure.

The sharp paramagnetic(PM)/ferromagnetic(FM) phase transition in $La(FeSi)_{13}$ based compounds was recently re-investigated by several research groups [4] [5] and large ΔS_{iso} with low magnetic/temperature hysteresis were reported. For this reasons the compounds still attract attention towards their use as active refrigerators in magneto cooling cycles. Many studies on the structural, magnetic and electronic properties demonstrated the first order nature of the phase transitions [6] [7] with concurrent sharp jump in magnetization (from PM to FM) and large negative lattice expansion [5] at the Curie point. To make the compounds suitable for applications, Fe atoms can be partially substituted by Co, to adjusts the Curie point towards higher temperatures (ambient), producing however a weakening of the first order nature of the transition [8].

A first order transition is characterized by an intrinsic latent heat decoupled from the continuous variation in the specific heat of a material. Since irreversibility is the cause of thermal and magnetic hysteresis when cycling MCE samples across

the Curie point, its origin can be investigated with dedicated calorimetry experiments. Many results directed on shape and critical sizes of the materials suggested the fundamental role of micro structure [9] in the hysteresis determination. However, these measurements, which can characterize the MCE properties of a material, provide volume informations, thus they make hard to distinguish between multiple contributions coming from the micro scale. On the other side, Magnetic Force Microscopy (MFM) [10] and scanning Hall probe imaging techniques [11] have been already applied for this purpose, showing that single sites behaviour can be quite different from the volume response. For this purpose, in the present work, we explore the local magnetic response at the surface of the compound $La(Fe_{0.9}Co_{0.015}Si_{0.085})_{13}$ using a Magneto Optic Imaging technique with Indicator Film (MOIF). As we already showed previously [12], the technique is able to dynamically follow the magnetic phase transition across an entire surface of a sample without loosing micro scale resolution on single sites, thus can be used to clarify some aspect related to local properties of the compound.

The paper is organized as follows. We first provide the necessary information to understand the MOIF technique and its application to magnetic materials. In the section results we show the quantitative data collected for different temperatures across the transition and we discuss the magnetic properties of defects and of the main phase. Finally we provide an interpretation of different dynamics observed in the compound when crossing the T_c based on previous results.

2. Material and measurement method

Polycrystalline Co substituted $La(Fe_xCo_ySi_{1-x-y})_{13}$ with x=0.9 and low Co content of $y = 0.015$ and $T_c = 200K$ was

prepared by powder metallurgy at Vacuumschmelze GmbH and CoKG [8]. The elemental analysis was performed by energy dispersive X-ray spectroscopy in a Scanning Electron Microscope (SEM) on a polished surface of the sample. Figure 1 shows a representative area of the sample and the distribution of the constituent elements based on their X-ray characteristic energies. Two secondary phases can be distinguished from the La-Fe-Co-Si matrix: αFe grains with size of 5 - 10 μm and a La-O-rich phase with bright contrast in backscattered electrons images [13] which might be also re conducted to the (1:1:1) phase of peritectic reaction: $\alpha Fe + LaFeSi(1:1:1) \rightarrow La(Fe, Si)_{13}$ [14]. The carbon-enriched spots are likely associated with diamond debris and organic matter accumulation in the holes of the sample, resulting from the sample polishing process.

For the MOIF measurements, we fixed the sample on the cold finger of a cryostat with a transparent window. The thermal contact was completed by silver paint between the bottom surface of the sample and a flat disc of thin aluminium positioned on the top of the cold finger. A cernox thermometer is inserted between the aluminium disc ant the cold finger to control the temperature of the sample. The technique [15][16] permits to visualize the stray field distribution at the surface of a magnetized object and is based on the use of garnet imaging films [17], which are sensitive to the out of plane component of the magnetic induction above the sample surface and some μm below it. The imaging film is a single crystal of Bismuth-Luthetium substituted iron garnet (BIG), deposited by liquid phase epitaxy on an optical substrate (Gadolinium-Gallium garnet) and equipped with a thin mirror (Ag) to amplify the signal. The BIG (Verdet constant $V = 30° \, kOe \, cm^{-1}$) is placed on the polished surface of the sample. As the magnetization inside the garnet rotates due to the stray field produced by the sample, the light polarization changes according to Faraday constant of BIG. Real time images can be recorded but they need to be calibrated for each temperature of measure subtracting a reference background ($H_{ext} = 0$), the response of the garnet to H_{ext}, and considering the polarizer angle with respect to the BIG surface.

3. Experimental

3.1. Field sweeps at fixed temperature

We identify different phases by comparison of MOIF images at temperatures above and below T_c; in figure 2, we show on the same scale, the optical image of the sample and the two magnetic contrasted MO images. The optical image (a) indicates the presence of holes which mainly correspond to the darker spots in the MO (c) when the sample is in its ferromagnetic phase. In the PM phase, figure 3 (b), the holes are not visible any more, while bright random spots origin from magnetic grains corresponding to the αFe phase identified with the SEM.

The analysis has been performed on sets of frames taken at fixed temperatures while sweeping the external magnetic field between -75 and 75 mT. The measured z-component induction's field is given by:

$$\mu_0 H^z_{meas} = \mu_0(H^z_{ext} + H^z_d), \tag{1}$$

the last term representing the dipolar field of the sample. Since the BIG is situated on top of the sample, we obtain a measure of the z-component of the local stray field present above the surface, H^z_{meas}. This field is dependent on the z-component of the magnetization according to magneto static equations. We collected and modelled the hysteresis loops at each pixel position across the sample surface. Based on phenomenological observation we used an hyperbolic tangent of the external applied magnetic field to fit the loops. We thus extract two parameters: the first, proportional to the external field and the second one, b, proportional to the cube of the external applied field.

$$H^z_{meas} - H^z_{ext} \approx a \cdot H^z_{ext}(z) - b \cdot (H^z_{ext}(z))^3 \tag{2}$$

The linear coefficient is conductible to the magnetic susceptibility of the sample $a = \chi_z$, while b is a correction factor. In Figure 3 (c) (d) we show the maps of χ_z for each pixel across the surface at temperatures above (T = 215 K) and below T_c (T = 185 K). These maps and their statistical distributions (figure 3 (a)(b)) permit to recognize two phases when $T > T_c$: the main (1:13) MCE phase of the sample which behaves as a paramagnet with low $\chi_z = 0.09$ and a second ferromagnetic phase of the αFe grains ($\chi_z = 0.78$). When we performed the same local statistical analysis at $T < T_c$, we clearly see a drastic change of the χ_z of the MCE phase which overlaps with the value of the ferromagnetic grains, respectively we found mean values of 1.54 and 1.37. Moreover, at this temperature, we found local minima values of $\chi_z \approx 0.95$ randomly sparse at surface which represent the holes or local sites where the transition do not occurs above 185 K.

In table I we summarizes the values of χ_z at T = 185 K and 215 K for the three different magnetic phases individuated: MCE (1:13) main phase, αFe grains and magnetic holes.

phases	χ_z	
	185 K	215 K
MCE phase	1.54	0.09
αFe	1.37	0.78
holes	0.95	0.10

Table 1: Resume of the values of the linear coefficient $a = \chi_z$ calculated for different phases and defects above (215 K) and below (185 K) the T_c.

The values of χ_z have been calculated as the mean value of the statistical distributions of local pixels (grains). Both αFe and holes grains represent a fraction below the 2% of the total sample surface. As we already say, at T = 185 K, the statistical distributions of the main MCE phase and αFe grains seem to collapse to a similar value. This can be a confirmation of what was already observed in [10], where was found a controversial behaviour in the ferromagnetic X-ray magnetic dichroism signal of isolated ferromagnetic grains present at the surface, which disappears below the Curie temperature. Above T_c the Fe grains are ferromagnetic and their stray field is observed clearly. Below T_c the matrix also become ferromagnetic, and the flux of the Fe grains is closed in the matrix , therefore is not observable by MOIF.
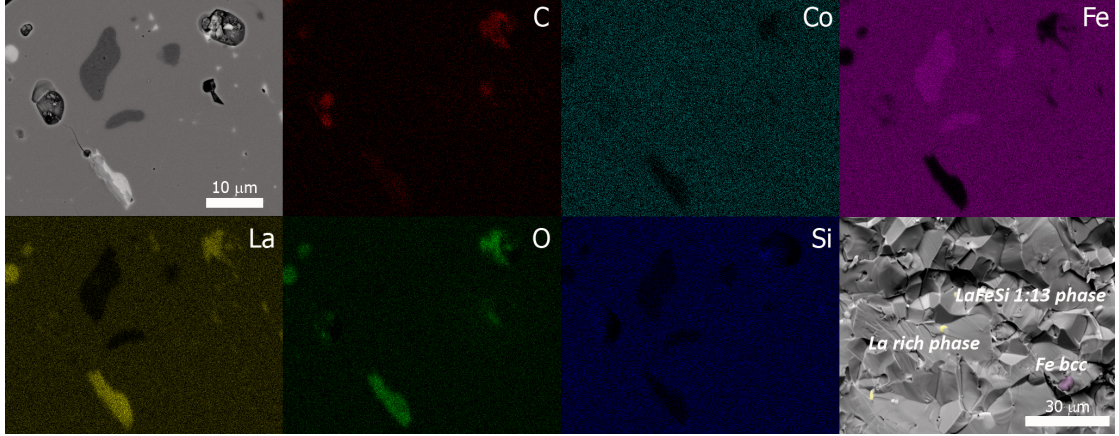
2

Figure 1: SEM backscattered electrons image of sample surface and elemental X-ray maps of the area; the characteristic X-ray energies of selected elements (C, Co, Fe, La, O, Si) are represented in false colors. Last image shows fracture surface of the sample where grains of the MCE phase are in grey and other phases are highlighted with the same colors of the X-ray maps.
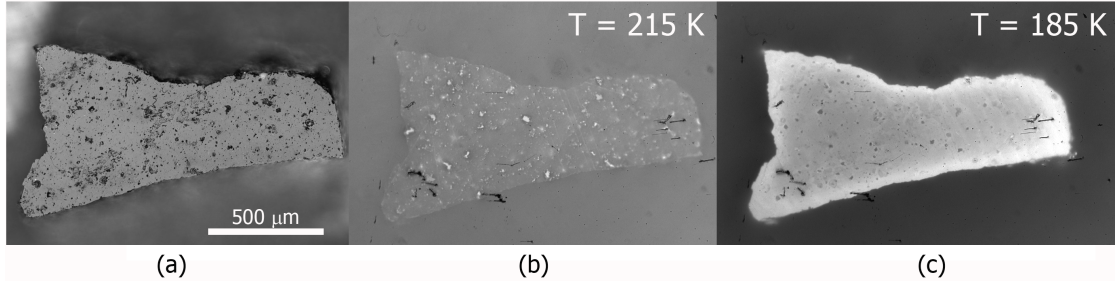

Figure 2: (a) Optical image of the entire sample. MO images of the magnetic contrast in the paramagnetic (b) and ferromagnetic phase (c).The dark spots in the FM phase of the sample (T = 185 K) mainly correspond to the holes of the optical image, while the bright spots in the PM phase (215 K) do not have a counterpart in the optical and FM images. In the MO images, the external magnetic field ($\mu_0 H_{ext} = 75\,mT$) is pointing out of the images plane.

Finally, from the statistical distributions in figure 3, we note that the holes individuated in the FM images have a large distribution of χ_z when T = 185 K, whether at the high temperature they behave as the rest of the PM phase. This is due to local stray fields of the ferromagnetic main MCE phase, which deviate due to the shape irregularities produced by holes at the surface.

3.2. Temperature sweeps at fixed field

Changing the temperature around the Curie point, we collected time/temperature sequences with resolution of ≈ 200 ms/ 11-15 mK/s to map the discontinuous transition from the PM to the FM state (and vice versa) of the magneto caloric phase. In these measurements, the external magnetic field was fixed at 30 mT perpendicular to the sample surface. We calculated from frames of the heating/cooling sequences the magnetic flux across the open top surface of the sample (at a distance of the garnet) computing the integral of the product of z-component of stray field measured with the orthogonal surface of the sample. Either in heating and in cooling, the growing of the new phase proceeds with some big jumps separated by almost continuous changes in the total magnetic flux. From figure 4 it is possible to recognise two big steps which correspond to two big part of the sample transforming: looking at the pictures, the right side

which transforms at lower T, and the left part which T of transition is almost 0.5 K higher. The real thermal hysteresis was obtained from a correlation of the measured data by the frame rate. This differences could be due to slight differences in the Curie temperatures or to the effect of thermal contact with the cold finger. However, thanks to the possibility to correlate the images of the whole surface with the total change in the magnetic flux, we notice, from some representative frames reported on the right of figure 4, that the two sides are not completely separated in temperature and some grains on the left start to transform with the big part on the right. Repeating the heating and cooling processes we observe that in both directions the nucleation of the new phase mainly start from the edges of the sample and move toward the centre. The big pinning events which stop the phase front are almost the same in heating and cooling and seems to be related to mechanical stresses or cracks in the sample produced by the lattice expansion. At the end of the experiment, the sample was in fact divided in many pieces. Our results, however, attempt to go behind these effect. Matching the frames of heating and cooling at which the MOIF images are similar, as showed in figure 4, the big jumps in the two directions are almost equal in temperature.

Thus, beside the big jumps, we observe that the low [18] hysteresis of this compound at the two sides of the sample changes from 20 to 4 mK. In spite of the slight faster temperature sweep
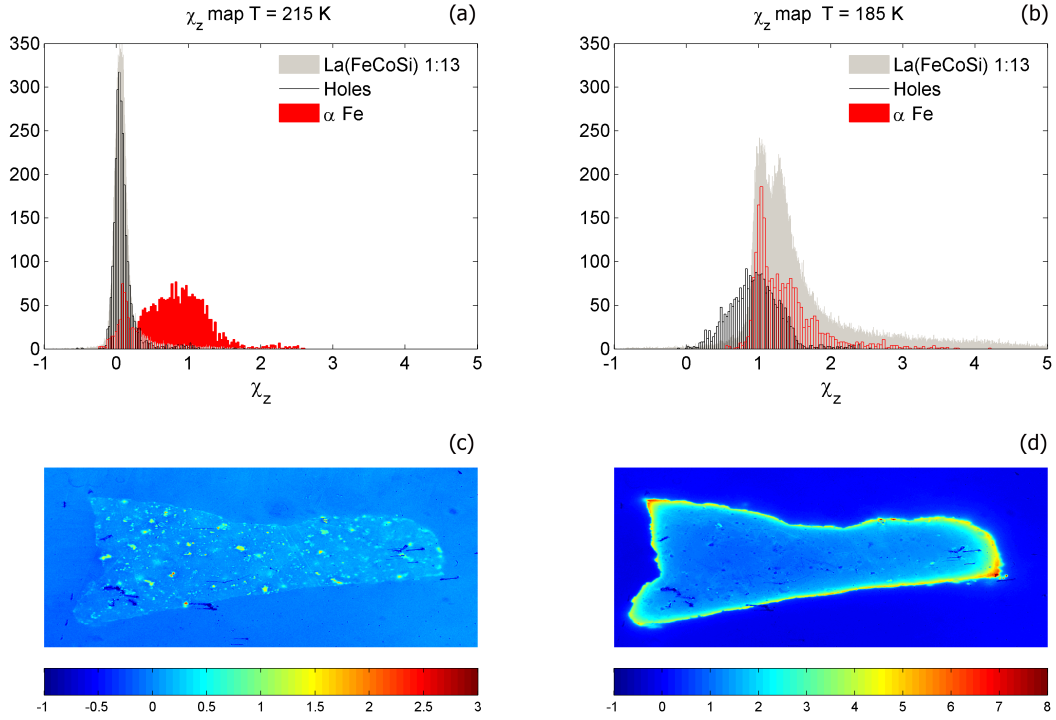
3

Figure 3: (a)(b) Statistics of the values of χ_z on Fe sites, holes and 1:13 MCE phase above and below the Curie temperature and (c)(d) respective local maps of the magnetic susceptibility across the sample. The values of counts of the MCE phase have been divided by 10^2 to make possible a comparison with the minor percentage of other phases (¡ 2% of the total surface).

rate, a longer time is spent in the linear part of the increasing total magnetic flux when the sample is cooled, whether, in the heating process, we observe a re-entrance of the total magnetic flux just after the strong de-pinning of the left grains. To explain the slower cooling transition we individuated from MO frames a particular behaviour of the FM front with respect to some αFe grains, around which, the FM transformation seems to be inhibited, an example is visible in figure 4 (frame h2) where an αFe grain in the middle of the sample is surrounded by the FM front. When the transition is completed and the magnetic flux is constant, as we pointed out in the previous section, the αFe grains disappear but magnetic holes in their vicinity are presents.

Revising the previous results, some of the holes which we have showed to posses a χ_z lower of the FM main phase can be regarded as 1:13 poor of Fe micro sized phases, with a lower Curie temperature and a lower total magnetic moment with respect to the main part of the compound. In our experiment, the magneto static field of magnetic phase front (FM) seems to interact with them and with αFe grains; beside the random nucleation process, the FM front advance seems to experience a magnetic friction.

4. Conclusions

The MOIF technique have been successfully applied to image the entire surface of $\approx 1000 \times 500$ μm^2 of a sample of the polycrystalline MCE compound $La(Fe_{0.9}Co_{0.015}Si_{0.085})_{13}$ above and below its Curie temperature ($\approx 198K$). The magnetic

properties of the main MCE (1:13) phase and of minor phases have been characterized and compared through the quantification of the local z-component of the stray field coming out from the sample. Observing the phase transitions with temperature, we evaluate different sources of hysteresis individuating some of the extrinsic factors which introduce disorder. We observe how the low thermal hysteresis of these class of compounds can be affected differently by the type of defects, structural or magnetic, which modify differently the energy landscape of the PM/FM front.

The size of the sample is crucial for our observation, structural defects or micro cracks give rise to the big jumps, these effects can be overcome by optimizing synthesis processes and by reducing the dimension of samples. On the other hand, the cooling nucleation process seems to be slowed down by the presence of magnetic impurities which introduce sources of random magnetic energy barriers and contribute to hysteresis. To avoid extrinsic hysteresis sources in the design of MCE material, a correct size evaluation of grains boundaries defects has to be take into account. The introduction of micro sized defects of different magnetic nature, which here is reported as a source of hysteresis, can be explored toward an optimization of the functional properties of compounds, it may be helpful to explore the type of energy barriers created by magnetic impurities by changing external field and temperature sweeping rate.
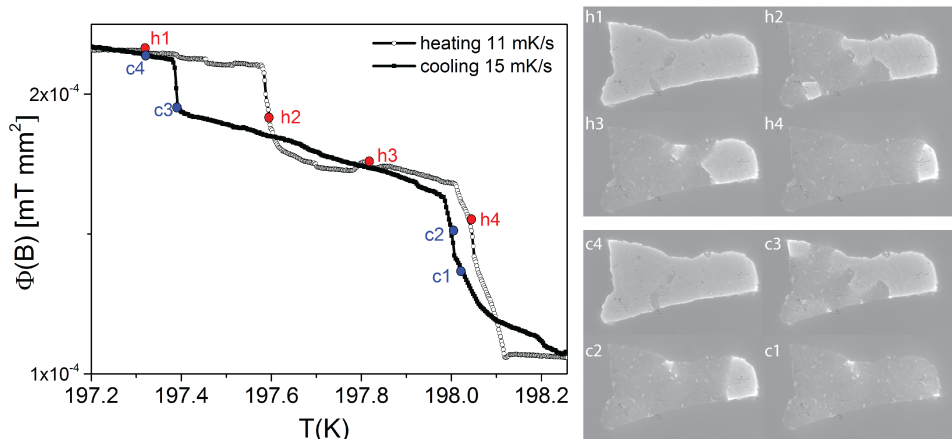
4

Figure 4: Left graph: magnetic flux integrated across the surface of the sample during a heating (11 mK/s) and a cooling (15 mK/s) transitions. The images on the right show the difference in the path followed by the surface ferromagnetic domains growth for the two temperature directions of the transition. In particular, h2 and c3, show that the energy barriers of bottom and up edges are very close to each other thus the one which disappear first is determinate by a random disordered process. An external biasing field of 30 mT is pointing out of the surface.

[1] K.A. Gschneidner, V.K. Pecharsky, Thirty years of near room temperature magnetic cooling: Where we are today and future prospects, International journal of refrigeration 31 (2008) 945-961.

[2] Aleksandr M. Tishin, Youry I. Spichkin, The magnetocaloric effect and its applications CRC Press (2003).

[3] E. Brück, O. Tegus, D.T. Thanh, H.H.J. Buschow, Magnetocaloric refrigeration near room temperature, Journal of Magnetism and Magnetic Materials 310.2 (2007) 2793-2799.

[4] S. Fujieda, A. Fujita, and K. Fukamichi, Large magnetocaloric effect in La(FexSi1-x)13 itinerant-electron metamagnetic compounds, Applied Physics Letters 81 (2002) 1276-1278.

[5] F. X.Hu, B. G. Shen, J. R. Sun, Z. H. Cheng, G. H. Rao, X.X. Zhang, Influence of negative lattice expansion and metamagnetic transition on magnetic entropy change in the compound LaFe11.4Si1.6, Applied Physics Letters 78.23 (2001) 3675-3677.

[6] F. X. Hu, X. L. Qian, J.R. Sun, G.J. Wang, X.X. Zhang, Z.H. Cheng, B.G. Cheng, Magnetic entropy change and its temperature variation in compounds La(Fe1-xCox)11.2Si1.8, Journal of applied physics 92.7 (2002) 3620-3623.

[7] A. Fujita, S. Fujieda, Y. Hasegawa, K. Fukamichi, Itinerant-electron metamagnetic transition and large magnetocaloric effects in La(FexSi1x)13 compounds and their hydrides, Physical Review B 67.10 (2003) 104416.

[8] M. Katter, V. Zellmann, G.W. Reppel, K. Uestuener Magnetocaloric Properties of Bulk Material Prepared by Powder Metallurgy, Magnetics, IEEE Transactions on, 44.11 (2008), 3044-3047.

[9] F. X. Hu, L. Chen, J. Wang, L.F.Bao, J.R. Sun, B.G. Shen, Particle size dependent hysteresis loss in La0.7Ce0.3Fe11.6Si1.4C0.2 firstorder systems, Applied Physics Letters, 100.7 (2012) 072403.

[10] V. Lollobrigida, V. Basso, F. Borgatti, P. Torelli, M. Kuepferling, M. Coïsson, F. Offi, Chemical, electronic, and magnetic structure of LaFe-CoSi alloy: Surface and bulk properties. Journal of Applied Physics, 115.20 (2014) 203901.

[11] K. Morrison, J.D. Moore, K.G. Sandeman, A.D. Caplin, L.F. Cohen, Capturing first-and second-order behavior in magnetocaloric CoMnSi0.92Ge0.08. Physical Review B, 79.13 (2009) 134408.

[12] M. Kuepferling, C.B. Bennati, F. Laviano, G. Ghigo, V. Basso, Dynamics of the magneto structural phase transition in La(Fe0.9Co0. 015Si0.085)13 observed by magneto-optical imaging. Journal of Applied Physics, 115.17 (2014) 17A925.

[13] J. Liu, M. Krautz, K. Skokov, T.G. Woodcock, O. Gutfleisch, Systematic study of the microstructure, entropy change and adiabatic temperature change in optimized LaFeSi alloys, Acta Materialia 59.9 (2011) 3602-3611.

[14] X. Chen, Y. Chen, Y. Tang, High-temperature phase transition and magnetic property of LaFe11.6Si1.4 compound, Journal of Alloys and Com-

pounds, 509.34 (2011) 8534-8541.

[15] F. Laviano, D. Botta, A. Chiodoni, R. Gerbaldo, G. Ghigo, L. Gozzelino, E. Mezzetti, An improved method for quantitative magneto-optical analysis of superconductors, Superconductor Science and Technology 16.1 (2003) 71.

[16] F. Laviano, R. Gerbaldo, G. Ghigo, L. Gozzelino, G. Lopardo, B. Minetti, E. Mezzetti, Stacking procedure for noise reduction in magneto-optical imaging, Physica B: Condensed Matter 403.2 (2008) 293-296.

[17] L.A. Dorosinskii, M.V. Indenbom, V.I. Nikitenko, Y.A. Ossip'yan, A.A. Polyanskii, V.K. Vlasko-Vlasov, Studies of HTSC crystal magnetization features using indicator magnetooptic films with in-plane anisotropy, Physica C: Superconductivity 203.1 (1992) 149-156.

[18] M. Kuepferling, C.P. Sasso, V. Basso, Rate dependence of the magnetocaloric effect in La-Fe-Si compounds, EPJ Web of Conferences EDP Sciences 40 (2013) p. 06010.